Turkish Journal of Electrical Engineering & Computer Sciences

http://journals.tubitak.gov.tr/elektrik/

Research Article

Turk J Elec Eng & Comp Sci
(2018) 26: 1190 – 1201

doi:10.3906/elk-1710-97

A new inset-fed UWB printed antenna with triple 3.5/5.5/7.5-GHz band-notched characteristics

Avez SYED*, **Rabah Wasel ALDHAHERI**
Department of Electrical and Computer Engineering, Faculty of Engineering, King Abdulaziz University, Jeddah, Saudi Arabia

Received: 08.10.2017 • **Accepted/Published Online:** 01.02.2018 • **Final Version:** 30.05.2018

Abstract: A novel low-profile inset-fed ultrawideband printed antenna with triple band-notched characteristics is proposed. Wide inverted U-shaped and crescent-shaped slots are used to achieve first and second notched bands in the 3.3–3.7 GHz and 5.1–5.9 GHz ranges for WiMAX and WLAN systems, respectively. Additionally, an altered ground plane with an open-ended L-shaped slot generated a third notched band in the 7.25–7.85 GHz range for downlink of X-band satellite communication systems. The center frequencies of the stop bands are adjusted by altering the parameters of corresponding slots. The antenna prototype is built on a 28 mm × 24 mm Rogers RT/duroid 5880 ($\varepsilon_r = 2.2$) substrate over a partial ground plane. Two concave circular curves were deployed on the patch with an inset feeding in order to obtain wideband performance in the 2.5–12 GHz (VSWR < 2) range with relatively good matching. The antenna prototype was fabricated and tested, and it was found to exhibit wideband performance, acceptable gain, and stable radiation pattern.

Key words: Inset feeding, notched band, printed antenna, ultrawideband

1. Introduction

The Federal Communications Commission granted permission in 2002 to use the 3.1–10.6 GHz frequency spectrum without the need for a license [1]. Following the granting of that permission, there has been an increasing research focus on designing ultrawideband (UWB) antennas that cover the 3.1–10.6 GHz spectrum. UWB antennas are the key elements in UWB communication systems since they have many interesting features such as low profile, low price, compact size, easy fabrication, omnidirectional radiation patterns, and ease of integration with printed circuit boards [2]. There are, however, significant challenges in designing UWB antennas. One of the main concerns is the presence of other narrow band systems like Worldwide Interoperability for Microwave Access (WiMAX), Wireless Local Area Network (WLAN), and X band satellite communication systems, all of them operating within the specified UWB band. Electromagnetic interference (EMI) from the aforementioned narrow bands degrades UWB system performance, and one method to eliminate EMI is to use filters that are designed to remove the interference from these narrow bands. However, the use of such filters, which are necessarily attached to a UWB antenna, increases system complexity and physical size. In addition, attaching filters to a UWB antenna increases the overall cost of the UWB system as well as making integration with system circuits more difficult. An easy method to address this issue would be to model antennas that have

*Correspondence: avez.ssyed@gmail.com

a band rejection function. Therefore, such antenna design can provide simple, compact, effective, low-profile, and low-cost UWB antennas.

In recent times, many methods have been discussed and implemented to obtain band-notched UWB antennas. Some UWB applications require that antennas have more than one rejection band. Various UWB antenna designs have been published including single band-notched [3–5], dual band-notched [6–8], and triple band-notched [9–16] designs. The basic technique for achieving notched band is to etch or cut apertures of numerous structures within the patch element [9–11]. In [12], triple band-notches were obtained by means of launching a stepped impedance resonator together with fork type stubs. In [13], stop-bands were created by loading three complementary codirectional split ring resonators in the radiating element. In [14], band notch function was obtained by adding open circuit stubs at the edge of the slot in addition to the defected ground structure. Triple notched frequency bands were generated in [15] by placing parasitic strips above the partial ground plane. A hollow cross loop resonator was packed within the aperture on top of the feed-line to create triple notched frequency bands in [16]. A significant disadvantage of most of these antenna types is that they are physically large with complex structure.

This paper proposes and presents prototype testing data for an inset-fed triple notched UWB antenna. The paper is arranged in the following way: Section 2 details the design of the antenna structure and gives a parametric analysis of each stop-band. Section 3 highlights the results along with a discussion. Lastly, Section 4 summarizes the findings of the presented work.

2. Antenna design

The multiple notched antenna presented in this paper is displayed in Figure 1. The fabrication of the prototype was carried on a 28 mm $\times$ 24 mm Rogers RT/duroid substrate material of thickness (h) 1.57 mm, loss tangent 0.0009, and permittivity (ε_r) 2.2. The antenna comprises a novel radiating element with a partial ground plane. Two concave circular cuts were deployed on the patch to obtain a wideband performance in the range of 2.5–12 GHz (VSWR $<$ 2). The antenna was fed using a 50 Ω microstrip inset feed line, which was symmetrical and had a width of 3 mm; the feed line achieved good impedance matching and its width is calculated by

$$w_f \approx \frac{h}{\pi}\left(A-1-\ln\left(2A-1\right)+\frac{\varepsilon_{eff}-1}{2\varepsilon_{eff}}\left[\ln\left(A-1\right)+0.39-\frac{0.61}{\varepsilon_{eff}}\right]\right), \quad (1)$$

where

$$\varepsilon_{eff}=\frac{\varepsilon_r+1}{2}, A=\frac{377\pi}{2Z_0\sqrt{\varepsilon_{eff}}}, \text{ and } Z_o=50\Omega.$$

The optimal dimensions of the proposed antenna, which were used to fabricate the antenna prototype for testing, are explained and shown in Table 1.

The proposed band-notched UWB antenna was designed in four simplified stages, as illustrated in Figure 2 (Designs I–IV); the VSWR curves for each of these design stages are shown in Figure 3. In the first stage, Design I is simulated, giving the required ultrahigh bandwidth (2.6–12.5 GHz); the ultrahigh bandwidth is provided by inset feeding and the two concave cuts. In the second stage, Design II, which has single band rejection in the 3.2–3.75 GHz band, was achieved by inserting a wide inverted U-shaped aperture within the radiating patch of Design I. In the third stage, an additional crescent slot was inserted into Design II, thus obtaining Design III, which was simulated to obtain two rejection bands: one at WiMAX, which was due to the inverted U-shaped slot, plus the other at WLAN (5.15–5.9 GHz), which was due to the crescent-shaped

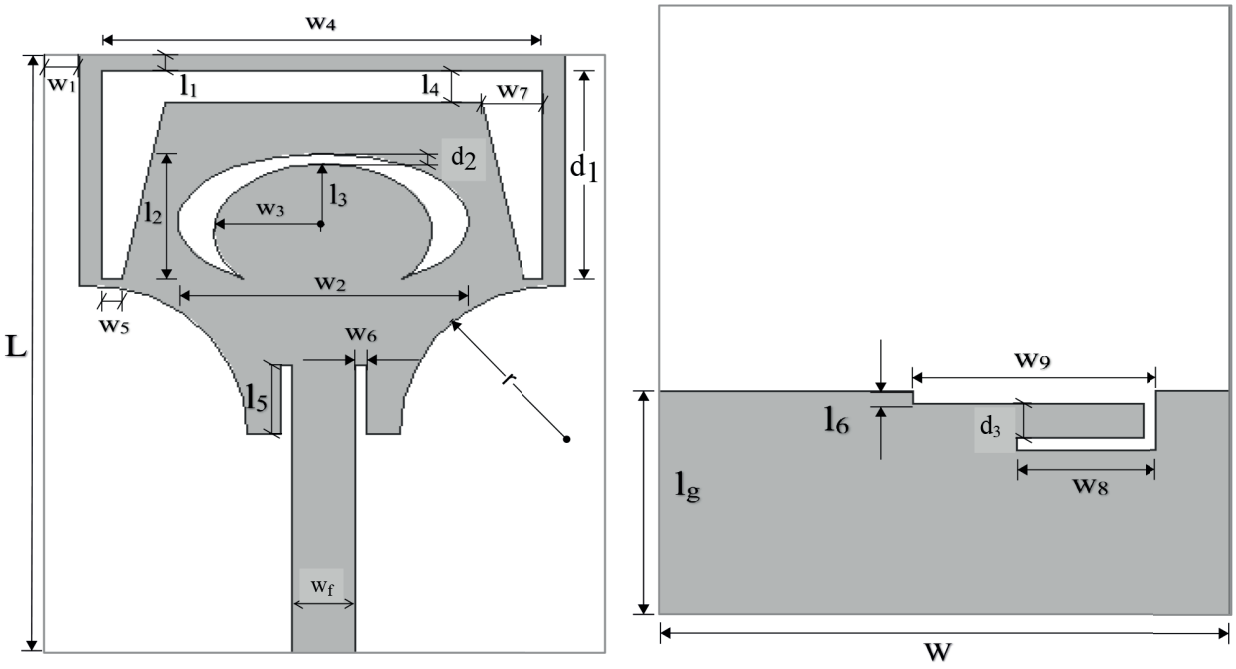

(a) (b)

Figure 1. Geometry of the antenna: (a) top layer, (b) bottom layer.

Table 1. Geometrical dimensions of the proposed antenna.

Parameters	mm	Parameters	mm
Length of substrate, L	28	Length of vertical groove of U-shaped slot, d_1	9.8
Width of substrate, W	24	Distance between centre of two ellipses, d_2	0.5
Width of feed line, w_f	3	Length of vertical groove of L-shaped slot, d_3	1.7
Radius of circular curve, r	7	Thickness of outer strip of patch, l_1	0.42
Height of substrate, h	1.57	Major axis of outer ellipse of crescent-slot,w_2	13
Inset length, l_5	3.22	Minor axis of outer ellipse of crescent-slot, l_2	6.5
Inset width, w_6	0.15	Length of open cut on ground plane, w_9	10.5
Gap, w_1	1.6	Thickness of L-shaped slot,l_6	0.5
Length of ground plane, l_g	10.48	Length of horizontal groove of L-shaped slot, w_8	6
Semimajor axis of inner ellipse of crescent-slot, w_3	4.87	Lower width of vertical groove of U-shaped slot, w_5	0.9
Semiminor axis of inner ellipse of crescent-slot, l_3	3.25	Upper width of vertical groove of U-shaped slot, w_7	2.8
Thickness of horizontal groove of U-shaped slot, l_4	1.5	Length of horizontal groove of U-shaped slot,w_4	19.8

slot. In the fourth and final stage, the third notch at 7.25–7.85 GHz was created by embedding an L-shaped slot in the partial ground structure, thus arriving at the required Design IV. It was observed that, for Design IV, since the notches were created independently, each notch had a high degree of isolation. Moreover, each rejection band was further tuned and optimized independently. Hence, it was possible to physically implement all three rejection elements (inverted U-shape, crescent-shape, and L-shape slots) either individually or in a single reference UWB antenna. The comparison of different stages of the proposed antenna is shown in Table 2.

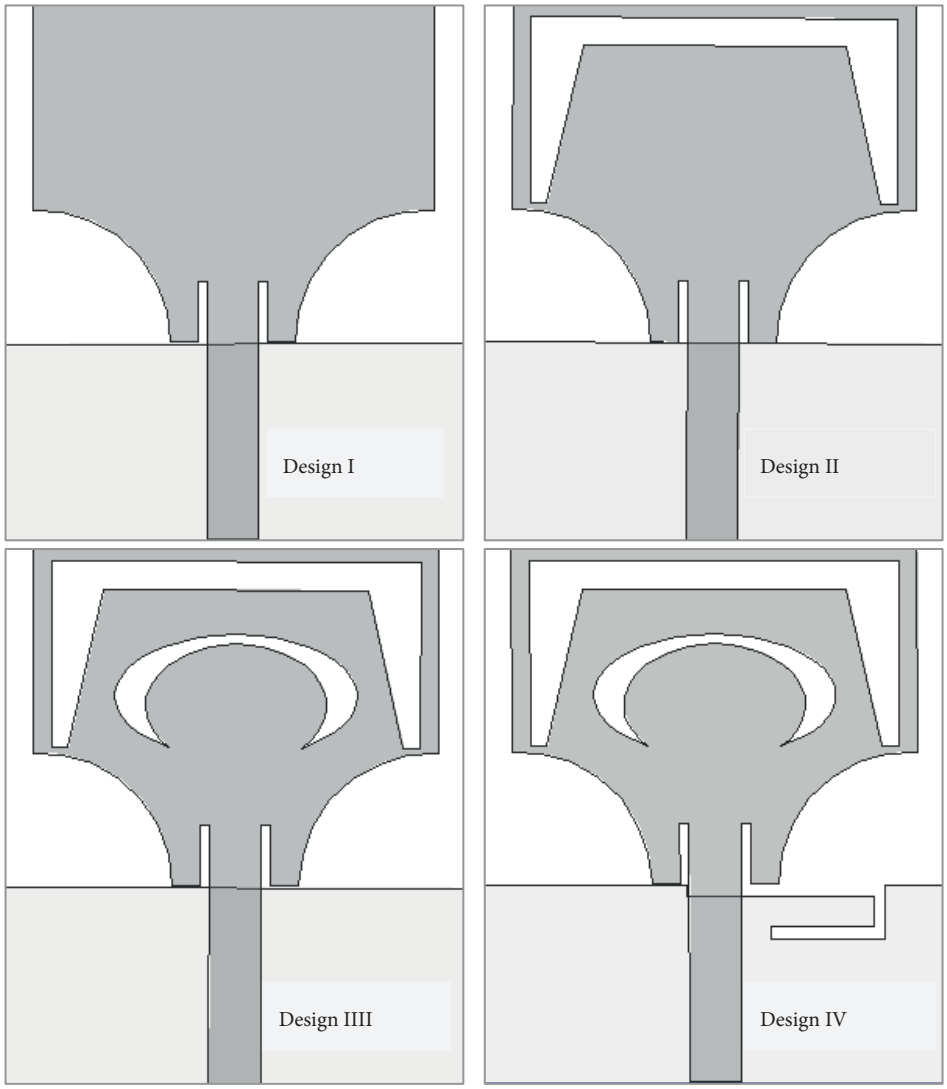

Figure 2. Four different design stages. Design I: UWB antenna. Design II: Single band-notched antenna. Design III: Dual band-notched antenna. Design IV: Proposed triple band-notched antenna.

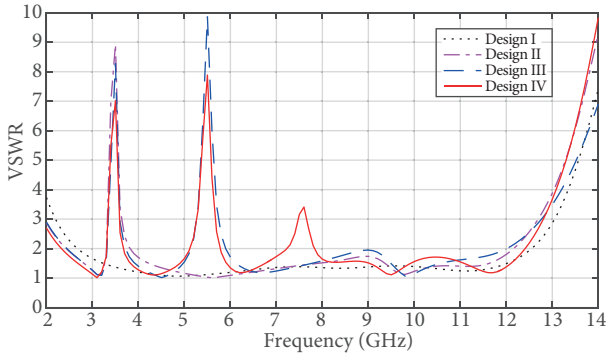

Figure 3. VSWR curves for the four different design stages.

Table 2. Comparison of different stages of the proposed antenna.

Features	Design I	Design II	Design III	Design IV
Pass band (GHz)	2.6–12.5	2.4–12	2.4–12	2.5–12
VSWR	1.3	1.4	1.5	1.4
Stop-bands	–	Single	Double	Triple
Slots	–	U-shaped	U-shaped/crescent	U-shaped/crescent/L-shaped
Notch frequency (GHz)	–	3.5	3.5/5.5	3.5/5.5/7.5
Notch bandwidth (GHz)	–	3.2–3.75	3.3–3.7/5.15–5.9	3.3–3.7/5.1–5.9/7.25–7.85
Size (mm^2)	28 × 24	28 × 24	28 × 24	28 × 24
WiMAX stop band	×	√	√	√
WLAN stop-band	×	×	√	√
X-Band downlink Stop-band	×	×	×	√

2.1. Inverted U-shaped slot

The very first stop-band, located at $f_{stop1} = 3.5$ GHz, was generated with the help of a wide inverted U-shaped aperture into the patch; this slot is approximately half wavelength and its length is given by

$$L_1 = [2\,(d_1) + w_4 - 2(w_7 - w_5)] = \frac{c}{2f_{stop1}\sqrt{\frac{\varepsilon_r+1}{2}}}, \tag{2}$$

where $c = 3 \times 10^8$ m/s. The center frequency f_{stop1} of the stop-band (3.3–3.7 GHz) can be adjusted by varying the length d_1 as illustrated in Figure 4. By increasing d_1, the stop-band shifts to the lower frequency region (left-hand side of the plot) with greater rejection value. The best result is obtained at $d_1 = 9.8$ mm. According to Eq. (2), the calculated and practical lengths of the inverted U-shaped slot are 33.88 mm and 35.6 mm, respectively.

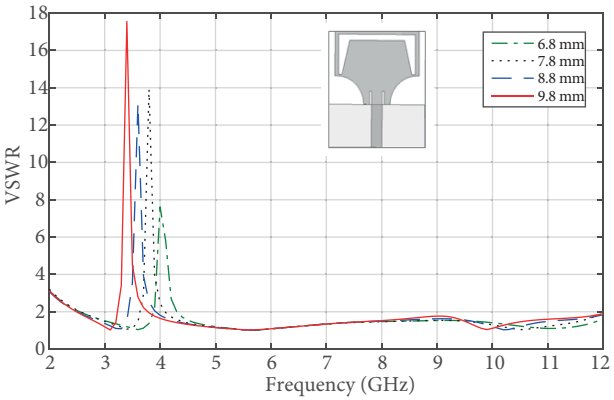

Figure 4. Variation of first notch with d_1.

2.2. Crescent-shaped slot

The second stop-band, located at $f_{stop2} = 5.5$ GHz, was produced with the help of a new crescent-shaped aperture. This crescent-shaped slot was designed by using two elliptical elements whose centers were separated

by a distance of 0.5 mm. This slot is approximately half wavelength and its length is given by

$$L_2 = \left[p_i \left(1 - \frac{d_2}{l_3}\right)\right] = \frac{c}{2f_{stop2}\sqrt{\frac{\varepsilon_r+1}{2}}}, \tag{3}$$

$$p_i = \pi \left[3\left(l_3 + w_3\right) - \sqrt{\left(3l_3 + w_3\right)\left(l_3 + 3w_3\right)}\right], \tag{4}$$

where P_i is the circumference of the inner elliptical (semimajor axis = w_3; semiminor axis =l_3) portion of the crescent slot. The center frequency of the stop-band (5.1–5.9 GHz) can be adjusted by varying the length d_2 as illustrated in Figure 5. By increasing d_2, f_{stop2} shifts slightly towards the higher frequency region (right-hand side of the plot). The best result is obtained at $d_2 = 0.5$ mm. According to Eq. (3), the calculated and practical lengths of the crescent-shaped slot are 21.56 mm and 21.79 mm, respectively.

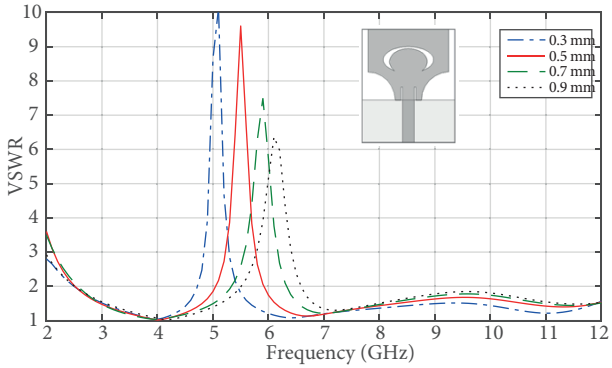

Figure 5. Variation of second notch with d_2.

2.3. L-shaped slot

The third stop-band, centered at $f_{stop3} = 7.5$ GHz, was created by inserting an open-ended L-shaped slot into the modified ground plane. This slot is approximately quarter wavelength and is given by

$$L_3 = [w_8 + l_6 + d_3] = \frac{c}{4f_{stop3}\sqrt{\frac{\varepsilon_r+1}{2}}}. \tag{5}$$

The center frequency of the notched band (7.25–7.85 GHz) can be adjusted by varying length d_3 as shown in Figure 6. By increasing d_3, f_{stop3} shifts slightly towards the lower frequency region. The best result is observed when $d_3 = 1.7$ mm. According to Eq. (5), the calculated and practical lengths of the L-shaped slot are 7.9 mm and 8.2 mm, respectively.

3. Results and discussion

The LPKF ProtoMat (S103) circuit board plotter was used to build the antenna prototype and its performance was determined with an Agilent network analyzer (N5225A). The antenna prototype for experimental measurements is shown in Figure 7. The measured VSWR curve aligns perfectly with the simulated VSWR and this phenomenon is best shown in Figure 8. The results clearly indicate that the antenna operates in the 2.5–12 GHz

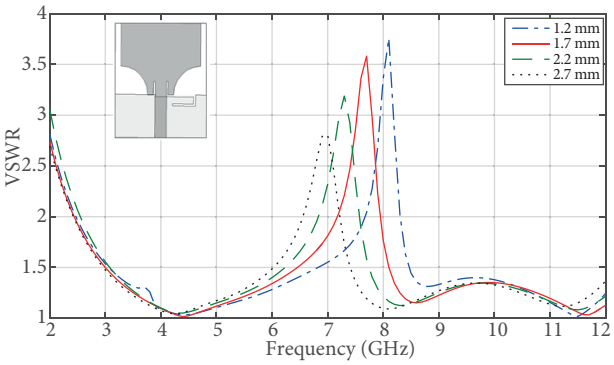

Figure 6. Variation of third notch with d_3.

(VSWR < 2) frequency band; this band covers the complete UWB band with triple band-notch characteristics. The three rejection bands are observed at 3.3–3.7 GHz, 5.1–5.9, and 7.25–7.85 GHz. There is a slight deviation of the experimental results from the simulation data; this is mainly caused by the SMA connector as well as the manufacturing threshold.

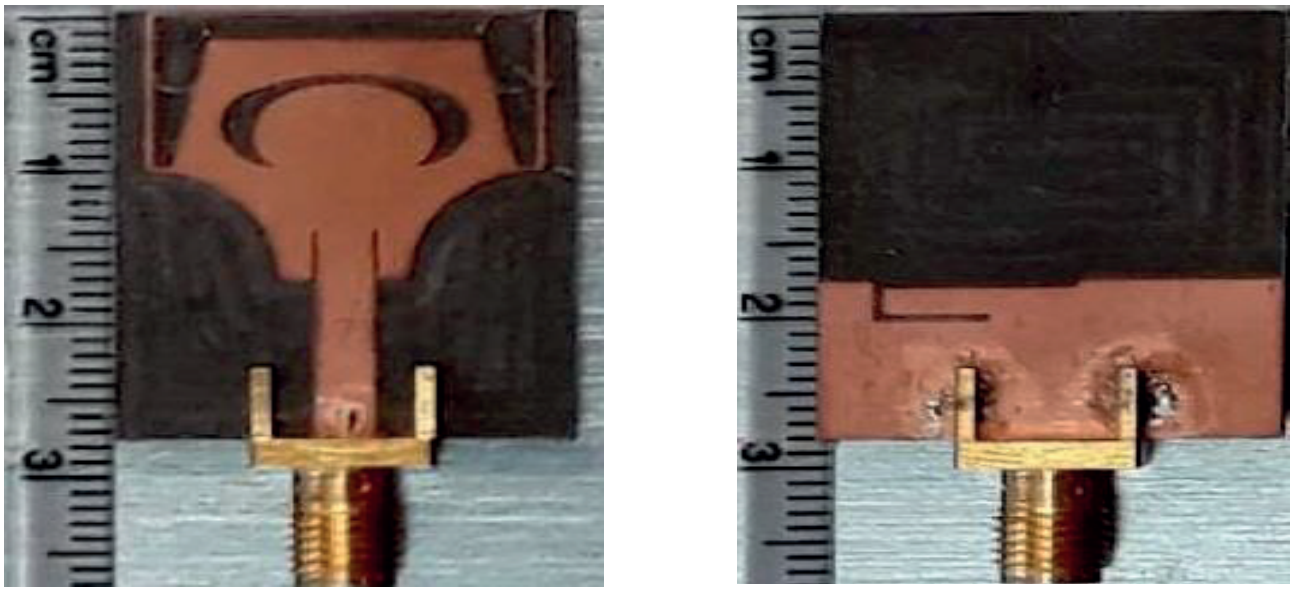

(a) (b)

Figure 7. Fabricated antenna prototype: (a) top view, (b) bottom view.

To further explore the band-notched function, the surface current distribution was simulated at each of the center rejected frequencies, as depicted in Figure 9. The current is rich on the inner and outer boundary of the wide inverted U-shaped slot at f_{stop1}, which clearly indicates that the energy is stored around this slot and not discharged into the surroundings. This proves the band rejection function. Moreover, the flow of the current on the edges of the patch is inversed to that in the slot. As a result, the whole effective radiations are lessened. The attenuation thus caused results in rejection of the 3.3–3.7 GHz frequency band, which, in turn, prevents potential interference from the WiMAX band. A similar effect is seen at the crescent (5.5 GHz) and L-shaped (7.5 GHz) slots. The frequency band of 5.1–5.9 GHz is rejected due to the high concentration of

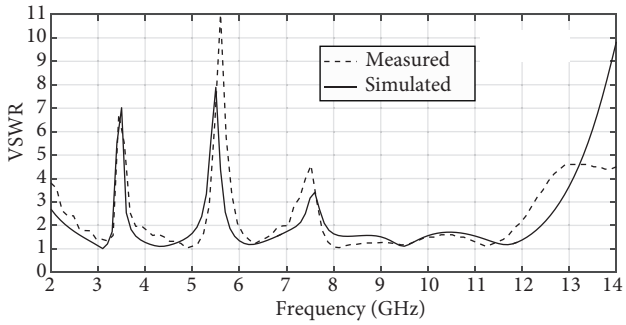

Figure 8. Simulated and measured VSWR curves.

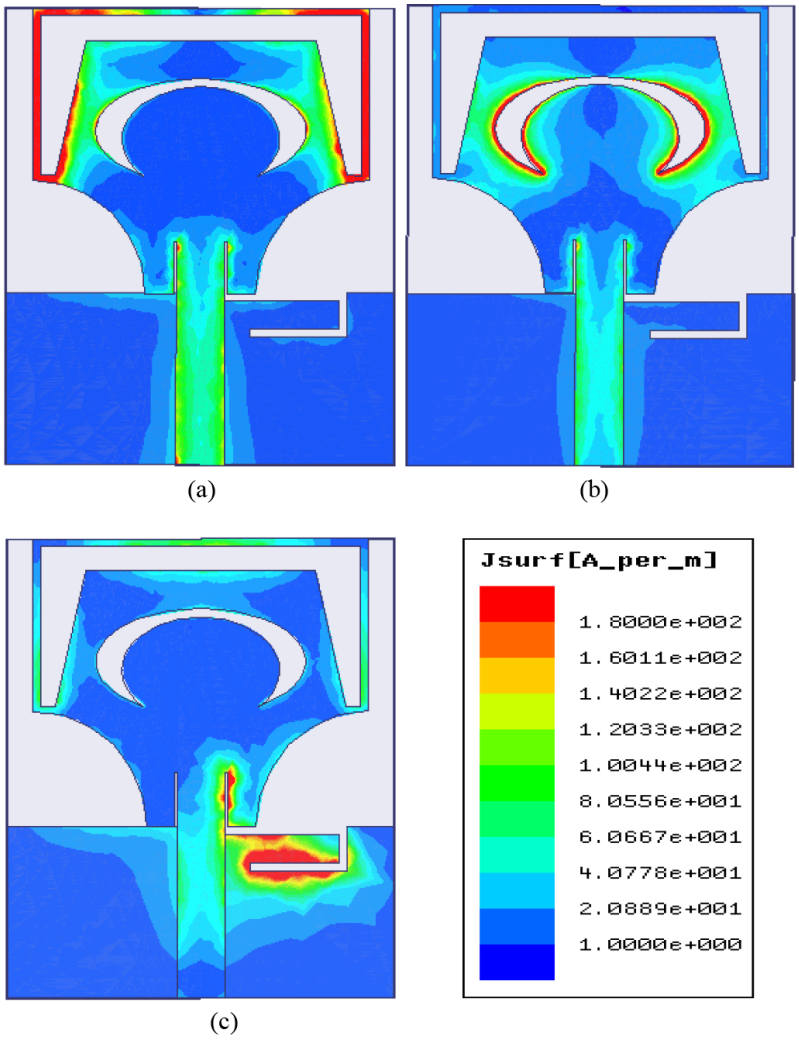

Figure 9. Surface current distribution on the antenna at (a) 3.5, (b) 5.5, and (c) 7.5 GHz.

current around the crescent slot with polarity of the current on the outer circumference being reverse to that on the inner circumference of the slot. The frequency band of 7.25–7.85 GHz is rejected due to more current around the L-shaped slot with polarity of current around this slot different from that on the partial ground plane. Also, the increase in slot length increases the current path, causing a shift in the stop-band. Moreover,

the electric field distribution at the notch frequencies is presented in Figure 10. It is seen that the field is uniformly distributed on the patch, except at the slots where it is highly concentrated. This accumulation of energy at the slots indicates that the energy is not radiated and hence leads to the rejection of frequencies 3.5, 5.5, and 7.5 GHz.

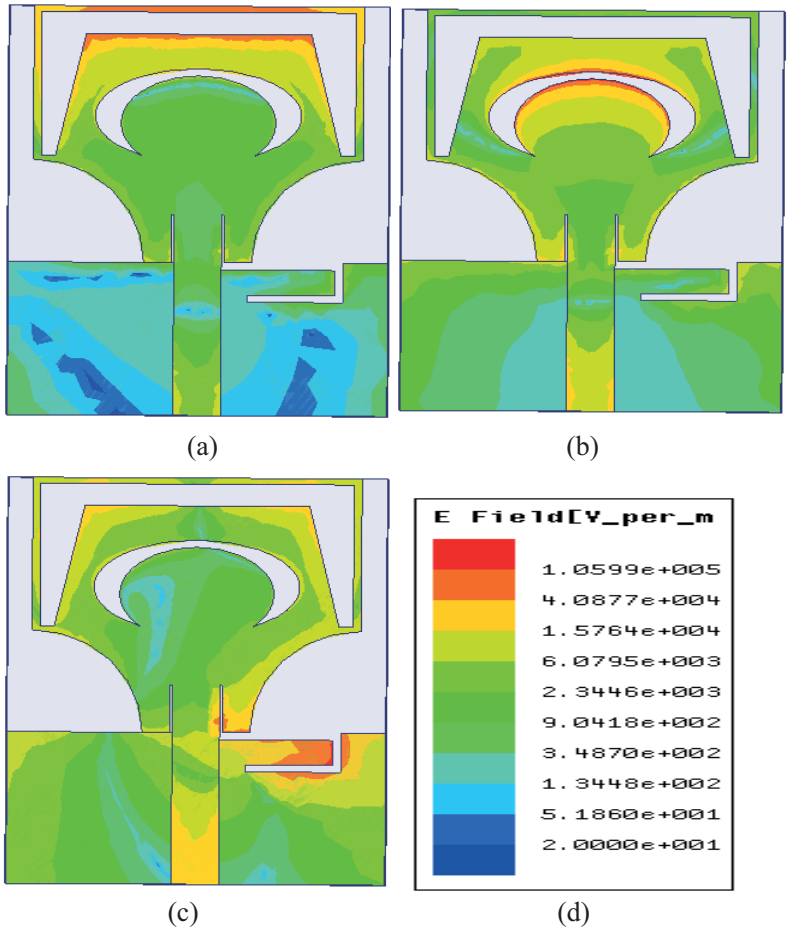

Figure 10. Electric field distribution on the antenna at (a) 3.5, (b) 5.5, and (c) 7.5 GHz.

Figure 11 presents the radiation performance of the designed prototype at various frequencies (3, 3.5, 4, 5.5, 6, 7.5, and 9 GHz). The antenna in the H-plane illustrates a stable and omnidirectional radiation structure. The radiation performance in the E-plane is slightly bidirectional, with two nulls. At the rejected frequencies the patterns are slightly distorted, but, overall, the patterns are stable over the whole UWB range. Table 3 displays the comparison of different antennas with the one proposed in this paper. The presented data clearly indicate that the proposed antenna has some excellent notch properties with relatively small size.

The designed antenna gain is as shown in Figure 12, with maximum peak gain of approximately 4.45 dBi. However, the antenna exhibits a sharp gain decrease in the 3.3–3.7 GHz, 5.1–5.9 GHz, and 7.25–7.85 GHz bands. This result shows that the antenna performs well in rejecting WiMAX, WLAN, and downlink of X-band links.

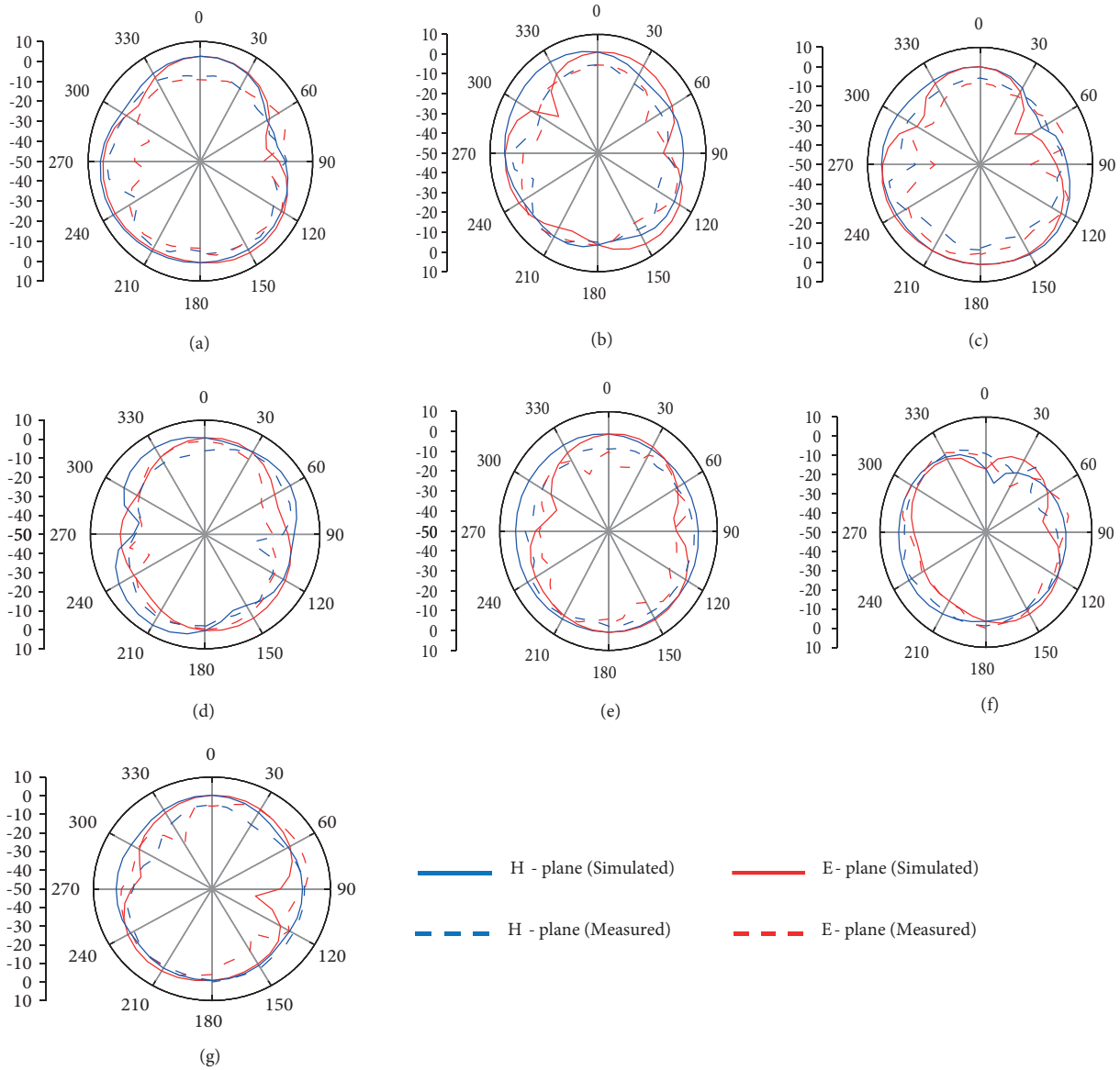

Figure 11. Measured and simulated radiation patterns of the proposed antenna at (a) 3, (b) 3.5, (c) 4, (d) 5.5, (e) 6, (f) 7.5, and (g) 9 GHz.

4. Conclusion

A straightforward inset-fed UWB antenna with three rejection bands has been implemented. The bandwidth of the fabricated prototype is 2.5–12 GHz, with rejection bands at the frequency bands of WiMAX (IEEE802.16), WLAN (IEEE802.11a/h/j/n), and downlink of X-band satellite systems. Three notches were generated by introducing U-shaped, crescent-shaped, and L-shaped slots. The resultant notches at 3.5, 5.5, and 7.5 GHz could be tuned and adjusted by appropriately varying d_1, d_2, and d_3, respectively. The analysis and comparison of the differently shaped antennas in the paper were performed. With its compact size (28 mm $\times$ 24 mm), the proposed antenna is among the smallest available triple notched band UWB antennas, making it easy to integrate into system circuits. This particular antenna is applicable as a multifunctional antenna to cut back

Table 3. Comparison of the proposed antenna with the existing antennas in literature. Here, λ_0 is the wavelength at the first resonance frequency.

Ref.	Dimension	Bandwidth (GHz)	Notch frequency (GHz)	Feeding technique
[9]	26 mm × 31.8 mm 0.30 λ_0 × 0.37 λ_0	2.8–12.6	3.5 (3.43–3.65), 5.2 (4.95–5.25), 5.7 (5.36–5.85)	Coplanar waveguide
[11]	30 mm × 30 mm 0.30 λ_0 × 0.30 λ_0	2.86–11.76	3.5 (3.25–3.75), 5.5 (5.1–5.8), 7.5 (7.25–7.75)	Microstrip
[12]	28 mm × 21 mm 0.28 λ_0 × 0.21 λ_0	2.8–11.3	3.5 (3.1–3.9), 5.68 (5.0–6.1), 7.48 (7.2–7.78)	Coplanar waveguide
[13]	30 mm × 25 mm 0.31 λ_0 × 0.26 λ_0	3.03–11.4	3.4 (3.3–3.6), 5.25 (5.15–5.35), 5.78 (5.725–5.825)	Microstrip
[14]	24 mm × 30 mm 0.22 λ_0 × 0.28 λ_0	2.6–12	3.5 (3.3–4.0), 5.3 (5.15–5.4), 5.9 (5.8–6.1)	Microstrip
[15]	30 mm × 22 mm 0.30 λ_0 × 0.22 λ_0	2.9–11	3.45 (3.26–3.71), 5.25 (5.15–5.37), 5.85 (5.78–5.95)	Microstrip
[16]	35 mm × 30 mm 0.34 λ_0 × 0.29 λ_0	2.55–12	3.5 (3.15–3.85), 5.7 (5.4–6.1), 8.2 (7.8–9.3)	Microstrip
Proposed antenna	28 mm × 24 mm 0.28 λ_0 × 0.24 λ_0	2.5–12	3.5 (3.3–3.7), 5.5 (5.1–5.9), 7.5 (7.25–7.85)	Inset-feed

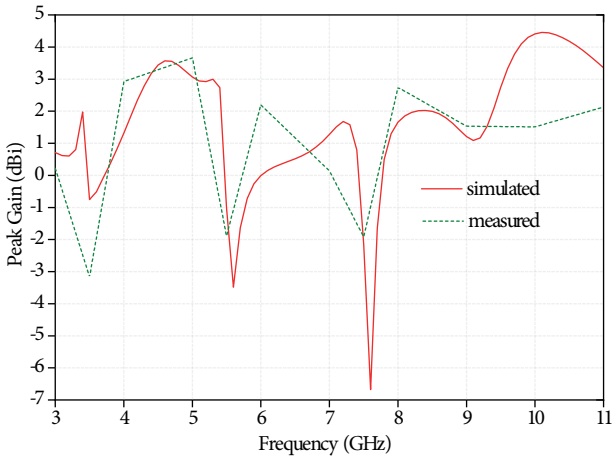

Figure 12. Gain curves of the designed antenna.

the number of antennas put in wireless devices for accessing multiple wireless networks. Moreover, the stable radiation patterns of the proposed antenna, along with its excellent notch characteristics, make it suitable for use in UWB applications.

References

[1] Federal Communications Commission. Revision of Part 15 of Commission's Rules Regarding Ultra-Wideband Transmission Systems, USA. First Report and Order. Washington, DC, USA: FCC, 2002.

[2] Balanis CA. Antenna Theory Analysis and Design. New York, NY, USA: John Wiley, 2005.

[3] Ojaroudi M, Ojaroudi N. Ultra-wideband small rectangular slot antenna with variable band-stop function. IEEE T Antenn Propag 2014; 62: 490-494.

[4] Syed A, Aldhaheri RW. A very compact and low profile UWB planar antenna with WLAN band rejection. Sci World J 2016; 2016: 3560938.

[5] Siddiqui YJ, Saha C, Antar YM. Compact SRR loaded UWB circular monopole antenna with frequency notch characteristics. IEEE T Antenn Propag 2014; 62: 4015-4020.

[6] Gao P, Xiong L, Dai J, He S, Zheng Y. Compact printed wide-slot UWB antenna with 3.5/5.5-GHz dual band-notched characteristics. IEEE Antenn Wirel Pr 2013; 12: 983-986.

[7] Jiang W, Che W. A Novel UWB antenna with dual notched bands for WiMAX and WLAN applications. IEEE Antenn Wirel Pr 2012; 11: 293-296.

[8] Azim R, Islam MT, Mobashsher AT. Dual band-notch UWB antenna with single tri-arm resonator. IEEE Antenn Wirel Pr 2014; 13: 670-673.

[9] Xu J, Wang G. A compact printed UWB antenna with triple band-notched characteristics. Microw Opt Techn Let 2012; 54: 2146-2150.

[10] Mohammadian N, Azarmanesh MN, Soltani S. Compact ultra-wideband slot antenna fed by coplanar waveguide and microstrip line with triple-band-notched frequency function. IET Microw Antenna P 2010; 4: 1811-1817.

[11] Mandal T, Das S. UWB printed plaque monopole antennas for tri-band rejection. Microw Opt Techn Let 2013; 55: 674-680.

[12] Zhang C, Zhang J, Li L. Triple band-notched UWB antenna based on SIR-DGS and fork-shaped stubs. Electron Lett 2014; 50: 67-69.

[13] Tang MC, Xiao S, Deng T, Wang D, Guan J, Wang B, Ge GD. Compact UWB antenna with multiple band-notches for WiMAX and WLAN. IEEE T Antenn Propag 2011; 59: 1372-1376.

[14] Liao XJ, Yang HC, Han N, Li Y. Aperture UWB antenna with triple band-notched characteristics. Electron Lett 2011; 47: 77-79.

[15] Islam MT, Azim R, Mobashsher AT. Triple band-notched planar UWB antenna using parasitic strips. Prog Electromagn Res 2012; 129: 161-179.

[16] Liu Y, Chen Z, Gong S. Triple band-notched aperture UWB antenna using hollow-cross-loop resonator. Electron Lett 2014; 50: 728-730.